Journal of Photochemistry & Photobiology, A: Chemistry 429 (2022) 113898

Contents lists available at ScienceDirect

Journal of Photochemistry & Photobiology, A: Chemistry

journal homepage: www.elsevier.com/locate/jphotochem

Second- and third-order nonlinear optical properties of mono-substituted terpenoid-like chalcones

Diego S. Manoel [a], André G. Pelosi [a], Leandro H. Zucolotto Cocca [a], Gustavo F.B. Almeida [b], Lucas F. Sciuti [a], Ruben D.F. Rodriguez [a], Luizmar Adriano Junior [c], Rosa S. Lima [d], Caridad Noda-Perez [d], Felipe T. Martins [d], Marcio A.R. Souza [d], Pablo J. Gonçalves [c,d], Tertius L. Fonseca [d], Leonardo de Boni [a], Cleber R. Mendonça [a,*]

[a] Instituto de Física de São Carlos – Universidade de São Paulo, Brazil
[b] Instituto de Física – Universidade Federal de Uberlândia, Brazil
[c] Instituto de Física – Universidade Federal de Goiás, Brazil
[d] Instituto de Química – Universidade Federal de Goiás, Brazil

ARTICLE INFO

Keywords:
Z-Scan technique
Hyperpolarizability
Chalcone
Nonlinear optics

ABSTRACT

Organic molecules exhibiting second and third-order nonlinear optical properties (NLOP) allow several applications in optics and photonics. Among the class of organic compounds, terpenoid-like chalcones derivatives constitute a suitable choice as nonlinear optical materials, given the possibility of obtaining a wide range of compounds that can be used in biophotonic applications. In this way, here we present a study of the first-order molecular hyperpolarizability and the two-photon absorption (2PA) cross-section of several terpenoid-like chalcones derivatives, aiming for applications in the therapeutic window. The 2PA spectra were evaluated employing the femtosecond tunable Z-Scan technique from 480 nm to 850 nm, and the first hyperpolarizability was determined at 1064 nm using the Hyper-Rayleigh scattering (HRS) technique. Moreover, the first-order molecular hyperpolarizability and the 2PA spectra were modeled by the sum-over-states (SOS) approach and undamped phenomenological model, respectively, providing new insights into the properties and compounds structure relationship. Results showed that substituent features, such as electron-donating or withdrawing ability, were associated with the 2PA cross-section magnitude. Regarding HRS results, it was possible to compare the difference of state dipole moment from both approaches, combining two experimental routes to determine photophysical parameters of non-fluorescent compounds, revealing the structure-relationship aiming the increase of the NLOP at the near-infrared region.

1. Introduction

Organic molecules exhibiting second and third-order optical nonlinearities are of foremost importance for developing applications in optics and photonics. Such properties can be exploited in optical power limiting [1], two-photon fluorescence imaging [2], 3D microfabrication [3,4], optical data storage [5,6], photodynamic therapy [7], and other photonic applications[8–14]. As it is known, the nonlinear optical properties depend on the molecular structure; the π-bridges allow an electronic delocalization leading to high odd nonlinearities [15], which can be further increased by adding withdrawing-electron or/and donor-electrons groups [16,17]. In this way, molecular frameworks that can be strategically modified are the research target for developing nonlinear organic materials.

Specifically, the chalcone backbone consists of two aromatic rings linked through a three-carbon $\alpha,\beta-$ unsaturated carbonyl system [18] that provides high π-electron delocalization owing to the double-bond between the rings. Owing to their intrinsic electron mobility, they are excellent candidates for nonlinear optical materials. Besides, chalcones are a well-known molecular class, which are naturally found in plants but are also synthesized in laboratories, with large biological applications as antibacterial [19] and anticancer [20]. In recent years, however, studies have shown that these molecules exhibit a high trend to crystallize [21], intense absorption in the UV/Vis region, and, most

* Corresponding author.
E-mail address: crmendon@ifsc.usp.br (C.R. Mendonça).

https://doi.org/10.1016/j.jphotochem.2022.113898
Received 1 November 2021; Received in revised form 28 February 2022; Accepted 5 March 2022
Available online 8 March 2022

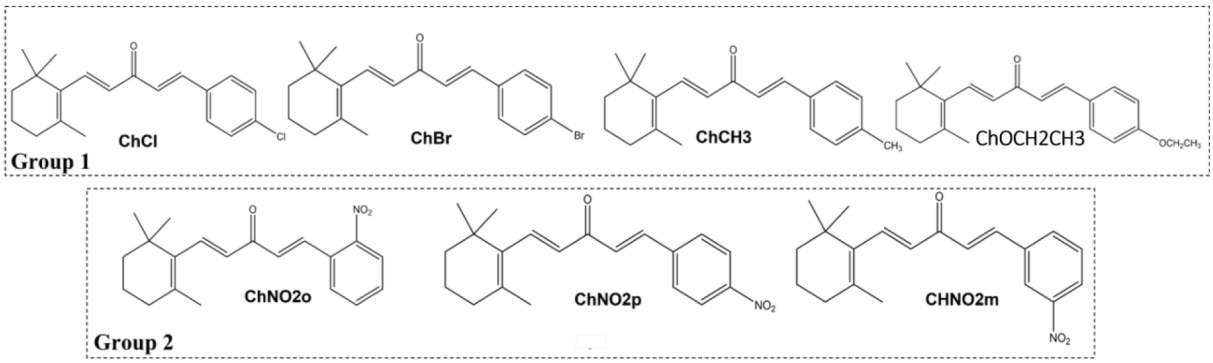

Fig. 1. The molecular structures of terpenoid-like chalcone derivatives.

importantly, high optical nonlinearities, including two-photon absorption (2PA) [22]. Because chalcones can be easily synthesized, they constitute a suitable choice as nonlinear optical materials, given the possibility of obtaining a wide range of compounds bearing the same molecular backbone. Therefore, studies on the nonlinear optical properties of chalcone derivatives provide insights on how changes in the molecular structures can enhance the optical nonlinearities towards the design of novel functional materials.

Terpenoids are hydrocarbons constituted by isoprene units (CH2 = C (CH3)–CH = CH2) which are found in plants, fungus, marine organisms, animals, oils, and other [23,24] While terpenes are simple hydrocarbons compounds, terpenoids are modified terpenes containing different functional groups and oxidized methyl groups. These changes provided diverse properties and functionalities such as biological activity and can be used for the treatment of many diseases, including cancer [25,26]. Besides, terpenoid-like molecules, such as carotenoids, present intense nonlinear optical properties with potential application in photonic devices[27–30]. Terpenes and terpenoids can be considered building blocks to develop new compounds for different applications.

Recently, new terpenoid-like chalcone derivatives with donor–acceptor (DA)-type structures were synthesized [31]. The structure of terpenoid-like chalcones is a hybrid compound with both structural frameworks, chalcone and ionone. β-ionone is a cyclic terpenoid compound, is the basic nucleus of retinoic acid, retinol, β-carotene, and vitamin A. Ionone derivatives occur in fruits, vegetables, and grains containing β-carotene [31]. Terpenoid-like structure raises the conjugation of chalcone frameworks and may be responsible for the increase of the structural stability of these compounds, which contribute to the development of crystals for nonlinear optical devices. Although these compounds have presented biological activity against tumor cells [32], linear and nonlinear optical properties of these compounds were not studied yet.

Here we studied the one-photon absorption (1PA), 2PA spectra, and the first-order molecular hyperpolarizability of several terpenoid-like chalcones with a common central molecular structure, differing from each other by the distinct substituents (Cl, Br, CH_3, OCH_2CH_3 or NO_2) placed at different positions of the main chalcone backbone. The 2PA cross-section spectrum was determined by the open-aperture Z-Scan technique [33,34] with excitation wavelength ranging from 480 nm to 850 nm, aiming, in specific, the determination of the 2PA magnitudes at the therapeutic window. The results were modeled by the sum-over-states approach that allowed determining photophysical parameters, such as transition dipole moments and the dipole moment difference between electronic states. It was observed a relationship of chalcones with groups Cl, Br, CH_3, and OCH_2CH_3 (electron donor substituents) linked to its core, displaying a higher 2PA cross-section than the ones with NO_2, in agreement with molecular orbitals calculations. Moreover, the Hyper-Rayleigh scattering (HRS) technique was used to determine the first-order molecular hyperpolarizability of the samples, which was phenomenologically modeled to determine the dipole moment difference. As a result of these approaches, excellent agreement between the dipole moments difference was obtained combining second- and third-order optical nonlinearities, indicating a new path to experimentally determine photophysical parameters for non-fluorescent compounds, which generally is a challenging task. Moreover, regarding NO_2 derivatives it was observed an increase of the dipole moments states difference from ortho, meta, and para-position leading to a considerable increase of the first hyperpolarizability.

2. Experimental section

Details about the synthesis of the seven terpenoid-like chalcone derivatives studied in this work, whose molecular structures are displayed in Fig. 1, can be found in Ref. [35]. The nomenclature used for the compounds is: **ChCl** ((1E,4E)-1-(4-chlorophenyl)-5-(2,6,6-trimethylciclohex-1-en-1-yl)penta-1,4-dien-3-one), **ChBr** ((1E,4E)-1-(4-bromophenyl)-5-(2,6,6-trimethylciclohex-1-en-1-yl)penta-1,4-dien-3-one), **ChCH3** ((1E,4E)-1-(p-tolyl)-5-(2,6,6-trimethylciclohex-1-en-1-yl)penta-1,4-dien-3-one), **ChOCH2CH3** ((1E,4E)-1-(4-methoxyphenyl)-5-(2,6,6-trimethylciclohex-1-en-1-yl)penta-1,4-dien-3-one), **ChNO2o** ((1E,4E)-1-(2-nitrophenyl)-5-(2,6,6-trimethylciclohex-1-en-1-yl)penta-1,4-dien-3-one), **ChNO2m** ((1E,4E)-1-(3-nitrophenyl)-5-(2,6,6-trimethylciclohex-1-en-1-yl)penta-1,4-dien-3-one, **ChNO2p** ((1E,4E)-1-(4-nitrophenyl)-5-(2,6,6-trimethylciclohex-1-en-1-yl)penta-1,4-dien-3-one.
Such compounds were divided in two groups to clarify the results presentation. **Group 1** is composed of **ChCl, ChBr, ChCH3** and **ChOCH3,** in which different peripherical groups (Cl, Br, Ch_3 and OCH_3) are linked at para-position of terpenoid-like chalcone backbone (Cl, Br, Ch_3 and OCH_3). The second one, **Group** 2, consists of **ChNO2o**, **ChNO2m** and **ChNO2p** with a nitro (NO_2) in *orto*, *meta* and *para* positions, respectively (Fig. 1). It should be mentioned that group 1 and 2 may exhibit a D-π-A-π-A and D-π-A-π-D, respectively. Therefore, group 1 and group 2 may have a charge distribution with dipolar-like and quadrupolar-like character, respectively.

Linear absorption measurements were carried out in dimethylsulfoxide (DMSO) solutions of the compounds with a concentration of approximately 5×10^{-5} mol/L, placed in a 1 mm optical path length quartz cuvette. A Shimadzu UV–Vis 1800 spectrometer was used to acquire the absorption spectrum at the UV–Vis-NIR spectral region. Two-photon absorption measurements were performed through the Z-Scan technique, in which the sample is translated around the laser's focus while its normalized transmittance (NT) is acquired. From such an experiment, the nonlinear absorption coefficient (β^{2PA}) is determined, and subsequently the 2PA cross-section (σ_{2PA}) by using $\sigma_{2PA} = h\nu\beta/N$, in which N is the density of molecules per cm^3 and $h\nu$ the photon energy. For the Z-scan measurements, we used a Ti: Sapphire chirped-pulse amplifier (CPA-2001, Clark-MXR Inc), centered at 775 nm with a repetition rate of 1 kHz and pulses of 150 fs. Such laser was employed as a pump source for an optical parametric amplifier (TOPAS, Light Conversion) producing 120 fs pulses with wavelengths between 470 and

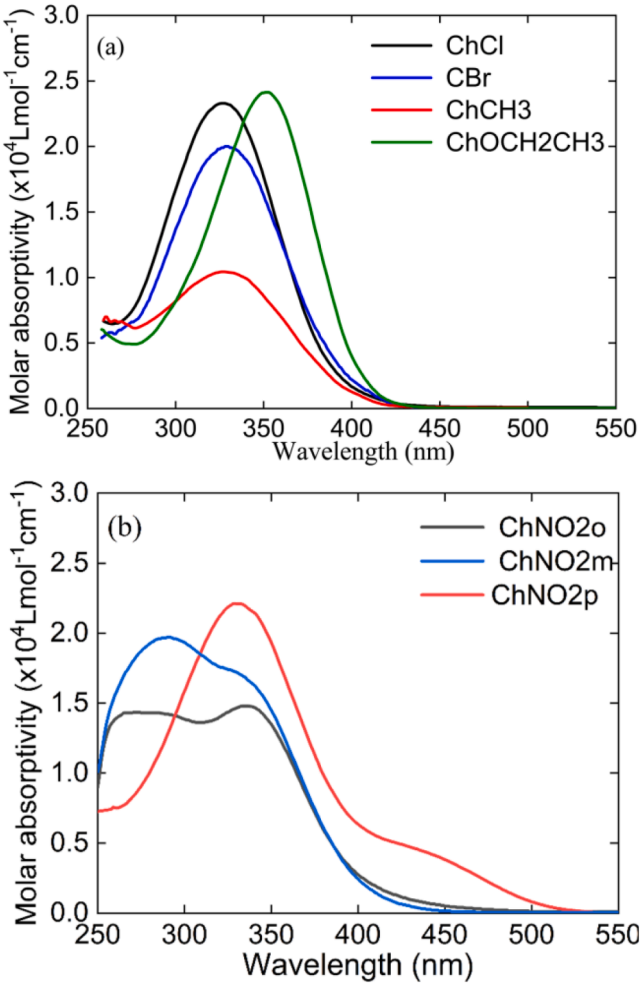

Fig. 2. The molar absorptivity of terpenoid-like chalcone derivatives in DMSO for a) group 1 and b) group 2.

Table 1
Spectral positions of the lower and higher energy transition of the chalcone derivatives in DMSO and gas-phase (G-P), oscillator strength of lower and higher energy band (f_{01} and f_{02}) in DMSO, determined with functional CAM-B3LYP/cc-pVTZ.

	CAM-B3LYP/cc-pVTZ				
Compound	λ_{01}^{G-P} (nm)	λ_{01}^{DMSO} (nm)	λ_{02}^{DMSO} (nm)	f_{01}	f_{02}
ChCl	312	334	–	1.05	–
ChBr	313	334	–	1.08	–
ChCH3	310	335	–	1.08	–
ChOCH2CH3	298	346	–	0.83	–
ChNO2o	306	331	268	0.83	0.24
ChNO2m	309	332	288	0.81	0.41
ChNO2p	320	344	–	0.96	–

2200 nm, allowing investigation of the 2PA in a wide spectral range. 2PA cross-section spectrum was measured for the studied compounds from 480 nm to 850 nm, with a 10 nm step. A spatial filter consisting of a 60 μm pinhole was employed to obtain a Gaussian profile for the excitation beam. A silicon photodetector is connected to a lock-in amplifier to collect and average (1000 laser shots) the NT of the sample for each z position.

To determine the first hyperpolarizability (β) the hyper-Rayleigh scattering (HRS) technique [36] was used. The experimental setup consists of an Nd:YAG Q-Switched mode-locked laser at 1064 nm working at 300 Hz. The laser pulse is composed of an envelope containing about 30 pulses (100 ps) separated by 13.2 ns. The laser is focalized in the sample with an intensity I(ω), and the nonlinear scattering intensity I(2ω) is acquired by a photomultiplier tube positioned perpendicularly to the laser beam. A bandpass filter at 532 nm is placed at the photomultiplier window to guarantee that the collected signal is from the nonlinear scattering. HRS experiments' signal is collected at 90° in relation to laser excitation. In such geometry and regarding the laboratory's coordinates (X,Y,Z) and molecular's coordinates (x,y,z), if the laser propagates in the X-direction and is vertically polarized in the Z-direction, the HRS signal can be written as $\langle\beta\rangle = \sqrt{\langle\beta_{ZZZ}^2\rangle + \langle\beta_{XZZ}^2\rangle}$, in which $\langle\beta_{ZZZ}^2\rangle$ and $\langle\beta_{XZZ}^2\rangle$ are macroscopic averages in which the first subindex (Z or X) is related to the state of polarization of the HRS signal. It is possible to rewrite $\langle\beta\rangle$ as a function of molecular first-order hyperpolarizability (molecular system reference) [22]. More details about the technique can be found in Ref [37]. The intensities relationship is given by:.

$$I(2\omega) = G\sum_{i=1}^{M} N_i\beta_i^2 I^2(\omega) \quad (1)$$

in which N_i is the molecular concentration, M is the number of components that could contribute to the HRS signal, is this case, M = 2 (DMSO and terpenoid-like chalcone derivative). However, experiments employing just the solvent (DMSO) were performed, and the HRS signal of DMSO can be neglected compared with the chalcone ones. Additionally, G is an instrumental factor that depends on the experimental setup. This constant can be determined using a sample with known β^{HRS}; in this work, we used as a reference para-nitroaniline (pNA) in DMSO ($\beta = 25.3 \times 10^{-30} esu$) [37]. Hence $\beta^{chalcone}$ is determined using

$$\beta^{chalcone} = \sqrt{\frac{\beta_{pNA}^2 \alpha_{chalcone}}{\alpha_{pNA}}} \quad (2)$$

in which $\alpha_{chalcone}$ and α_{pNA} are the angular coefficient of I(2ω) *vs* N_i plot, and they are given by $\alpha_{chalcone} = G\beta_{chalcone}^2$ and $\alpha_{pNA} = G\beta_{pNA}^2$. β values are usually presented in *esu* and the conversion factor from *SI* and atomic units to *esu* are given by 2.693×10^{20} cm^5 esu^{-1} and 8.641×10^{-33} cm^5 esu^{-1}, respectively [38,39]

Finally, TD-DFT calculations have been performed using the Gaussian09 program. The optimized geometries were obtained at the B3LYP/cc-pVTZ level in the gas phase and DMSO by using the polarizable continuum model (PCM) solvation model [40]. The vertical excitation energies at the optimized structures were obtained at the CAM-B3LYP/cc-pVTZ level.

3. Results and discussion

As depicted in Fig. 2, compounds of **Group 1** presented electronic transitions between 300 and 350 nm, while the ones from **Group 2** displayed two electronic transitions: for ChNO2o and ChNO2m, the higher and lower energy electronic transition is at around 270 nm and 350 nm, respectively. On the other hand, for ChNO2m, the higher energy electronic transition is at about 350 nm, and the lower one is at around 450 nm. Different features were observed at the lower energy band for each compound, such as spectral position and magnitude of molar absorptivity coefficient (ε) due to different withdrawing and donor-electron groups linked on the chalcone backbone.

All the compounds presented magnitudes of molar absorptivities (ε) around 2.0×10^4 L mol^{-1} cm^{-1}, except for **ChCH3** and **ChNO2o**, which displayed values of ε around 1.2 and 1.5 $\times$ 10^4 L mol^{-1} cm^{-1}, respectively. In fact, the chalcone backbone has attracted attention in 2PA.

studies due to its entirely conjugated moiety made up of alternated single and double bonds [22]. Besides, for **Group 1** (Fig. 2a) it was observed only one absorption band, while for **Group 2** (Fig. 2b), a second electronic transition, possibly owing to the strong electron-withdrawing character of NO_2 groups, was observed. The template

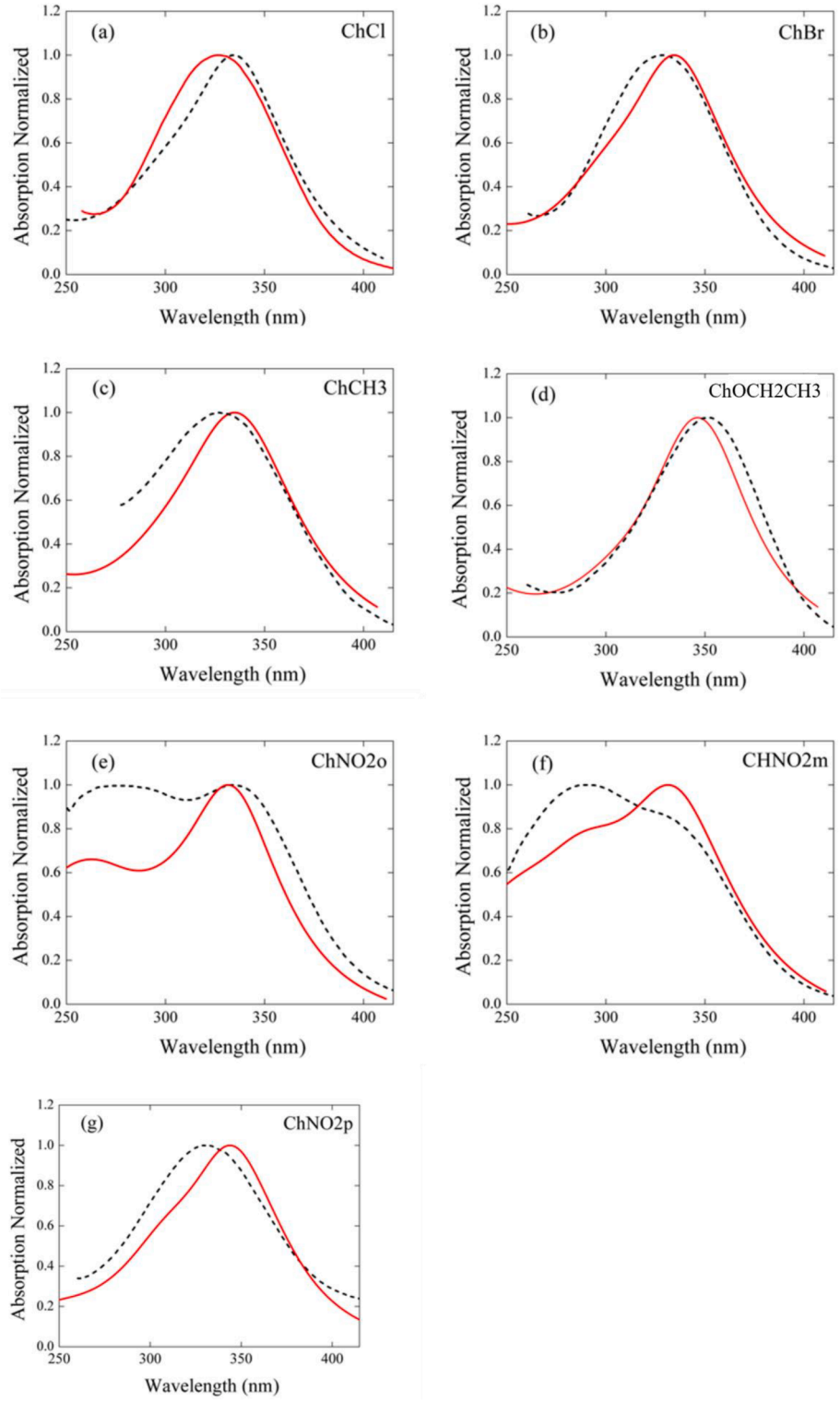

Fig. 3. Experimental (black dashed lines) and simulated (red continuous line) oscillator strength for the chalcone studied here.

compounds of **Groups 1** and **2** were those synthesized in high yields. The considerable decrease of ε for compound **ChCH3** may be related to the weak donor-electron character of CH_3 when compared to the stronger character of OCH_3 and the electron-withdrawing trend of Cl and Br. Analyzing the maximum absorption bands, the presence of Cl, Br, (acceptor-electron atoms), and CH_3 (weaker donor-electron group) substituents slightly affect the peak position. However, changing these substituents by OCH_3 (stronger donating-electron group) causes a pronounced experimental redshift of 23 nm. Such observation could be explained because the D-π-A (OCH_3-π-C = O) molecular structure increases the effective conjugation length (increase owing to the additional charge-transfer) compared to A-π-A, whose strong electron-withdrawing groups decrease effective conjugation length. In addition, a considerable shift of the lower energy band of **ChNO2p** (NO_2 at para-position) was verified, with a shoulder around 440 nm.

Table 1 shows TD-CAM-B3LYP/cc-pVTZ results for the electronic

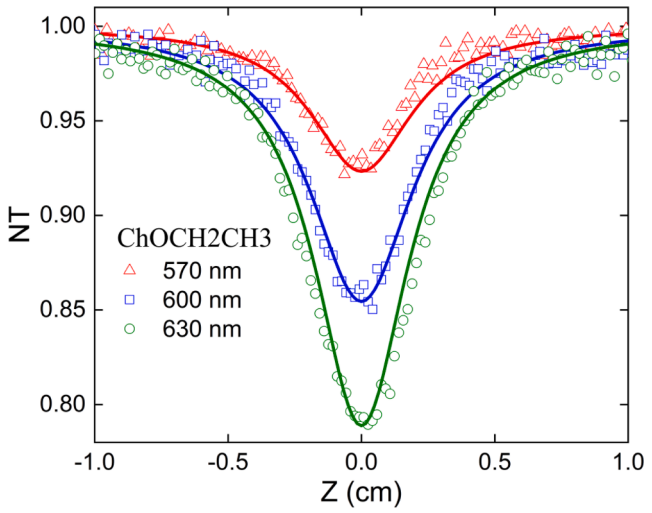

Fig. 4. Typical signal of Z-Scan technique for ChOCH3 compound.

transitions of the compounds in gas-phase (λ_{01}^{G-P}) and DMSO (λ_{01}^{DMSO}) as well as the oscillator strength of the lower (f_{01}) and higher (f_{02}) energy transition. For compounds of **Group 1,** the highest shift between gas-phase and DMSO was observed for **ChOCH2CH3** (48 nm), while the lowest one was observed for **ChBr** (21 nm). On the other hand, in compounds of **Group 2,** similar redshifts – **ChNO2o, ChNO2p,** and **ChNO2m** presented 25 nm, 24 nm, and 23 nm, respectively – were observed for all compounds, indicating that ortho, para, and meta substitution may have the same influence on it. The redshift observed in DMSO media may be understood owing to the energy-losses of the excited state to reach the stabilization of it (values of dielectric constant and linear refractive index of DMSO are 46.7 [41] and 1.47 [42], respectively.) Besides, the spectral width (considering a Lorentzian spectral width) was around 60 nm for all compounds studied in this work.

In Fig. 3, the normalized theoretical absorption spectra (red line) are compared with the corresponding experimental ones (black dashed lines) for the studied compounds. In such results, it was considered that molecules are dissolved in DMSO. A better agreement between the convoluted theoretical results with the experiment is achieved with a half-width at half-maximum between 60 and 70 nm. It is important to highlight that for **Group 2** theoretical results displayed two excited states closer to each other, while for **Group 1** just one was verified, which agrees with the experimental results.

The experimental 2PA cross-section values were determined through the tunable femtosecond Z-Scan technique. Typical signals for excitation wavelengths are displayed in Fig. 4. For all other compounds and wavelengths, the same behavior was observed.

The 2PA cross-section (2PACS) results displayed in Fig. 5 (open circles) revealed that all compounds presented a non-centrosymmetric charge distribution character, as the 1PA state is also accessed by 2PA. Besides, molecules of group 1 presented one 2PA allowed band at the near infrared region. For this group, **ChCl** compound displayed the largest 2PACS, with 32 GM. Compounds **ChBr**, **ChCH3,** and **ChOCH2CH3** presented similar 2PACS values of approximately 25 GM. In the case of terpenoid-like chalcone derivatives of **Group 2**, it was observed a particular behavior related to the –NO_2 group position. Two allowed 2PA bands were observed for –NO_2 at *ortho* and *meta* position, in which the highest energetic ones show approximately two folds of magnitude compared to the lowest ones. However, when –NO_2 is at *para* position, only one 2PA allowed band was obtained with the smallest 2PACS of all compounds. The absence of a 2PA lower energy band may be explained by the largest split of the states in comparison with *ortho* and *meta* derivatives, shifting the 2PA lower energy band to higher wavelengths. In the last years, nonlinear properties of diverse chalcones derivates have been evaluated [43], and the obtained values in the present work are close to the best values previously found [43].

To better understand the 2PACS spectra, we used quantum chemistry calculations (QCC) to determine the frontier molecular orbitals of the terpenoid-like chalcone derivatives studied here. Results showed that the lowest energy band originates mainly from the excitation of the lowest occupied molecular orbital (HOMO) to the highest unoccupied molecular orbital (LUMO), which correspond to a π-π* excited state. The frontier molecular orbitals are shown in Fig. 6. For terpenoid-like chalcone derivatives with Cl, Br, CH_3, and OCH_2CH_3 substituents (**Group 1**), the HOMO orbitals are mainly localized on the central conjugated open-chain and the aromatic ring; upon excitation, the LUMO orbitals also exhibit a similar distribution, but with a higher localization on the central moiety. In contrast, for the nitro derivatives (**Group 2),** the HOMO orbital is localized on cyclohexene, whereas the LUMO is localized on the nitrobenzene moiety, indicating an efficient intramolecular charge transfer. It is essential to mention that the NO_2 group has a more effective electron-accepting character than C═O, which may explain the unexpected decrease of 2PACS for compounds of **Group 2.** Also, based on the frontier molecular orbitals, the compounds can be separated into two parts, considering the carbonyl groups as the center: (i) the cyclohexene ring, which is the same for all compounds, and (ii) the para-substituted phenyl ring. The methyl radicals appended on cyclohexene are electron donors (D), while the C═O group is an acceptor (A) such that a D-π-A path comes from this six-membered ring. On the other side of the molecules, there is also a similar D-π-(A or D) structure, depending on the substituent (electron acceptor or donor group). For the compounds studied here, the incorporation of donor substituents rather than acceptor ones gives rise to a D-π-A-π-D structure, which can enhance nonlinear response resulting in improved 2PA cross-section. In other words, the D-π-A-π-D structure is more promising in terms of 2PA in our compounds due to cooperative electron donation to the central acceptor group, rather than a D-π-A-π-A structure where there are two acceptor groups competing for just one electron donor.

We have also modeled the 2PACS spectra of the studied compounds using the SOS approach (red lines – Fig. 5). Such a model considers the essential electronic energy levels which mainly contribute to nonlinear optical processes. For the compounds studied here, the energy diagram used in the SOS model is displayed in Fig. 7. Because for compounds of **Group 1** we verified only one electronic transition ($S_0 \rightarrow S_1$), the 2PA cross-section, in the context of the SOS model, is described by.

$$\sigma(\omega)_{2PA} = \frac{128\pi^5}{5(hcn)^2}L^4\left[\frac{(\Delta\mu_{01}^2\mu_{01}^2)G_{01}}{(\omega_{01}-\omega)^2+G_{01}^2}\right] \quad (3)$$

in which h is the Planck's constant, c is the light speed, n is the linear refractive index of the solvent, and L is the Onsager's field factor given by $3n^2/(2n^2+1)$.ω_{01}, $\Delta\mu_{01}$ and μ_{01} are the frequency transition, the dipole moments difference, and the transition dipole moment from the ground to the first excited state, respectively.

Owing to the presence of two excited states (S_1 and S_2) for compounds of **Group 2**, the 2PA cross-section is given by [44–47].

$$\sigma(\omega)_{2PA} = \frac{128\pi^5}{5(hcn)^2}L^4\left[\frac{(\Delta\mu_{01}^2\mu_{01}^2)G_{01}}{(\omega_{01}-2\omega)^2+G_{01}^2}+\frac{(\Delta\mu_{02}^2\mu_{02}^2)G_{02}}{(\omega_{02}-2\omega)^2+G_{02}^2}+\frac{\omega^2}{(\omega_{01}-\omega)^2+G_{01}^2}\frac{(\mu_{12}^2\mu_{01}^2)G_{02}}{(\omega-2\omega)^2+G_{02}^2}+\frac{(\Delta\mu_{02}\mu_{02}\mu_{01}\mu_{12})G_{02}}{(\omega_{02}-2\omega)^2+G_{02}^2}\right] \quad (4)$$

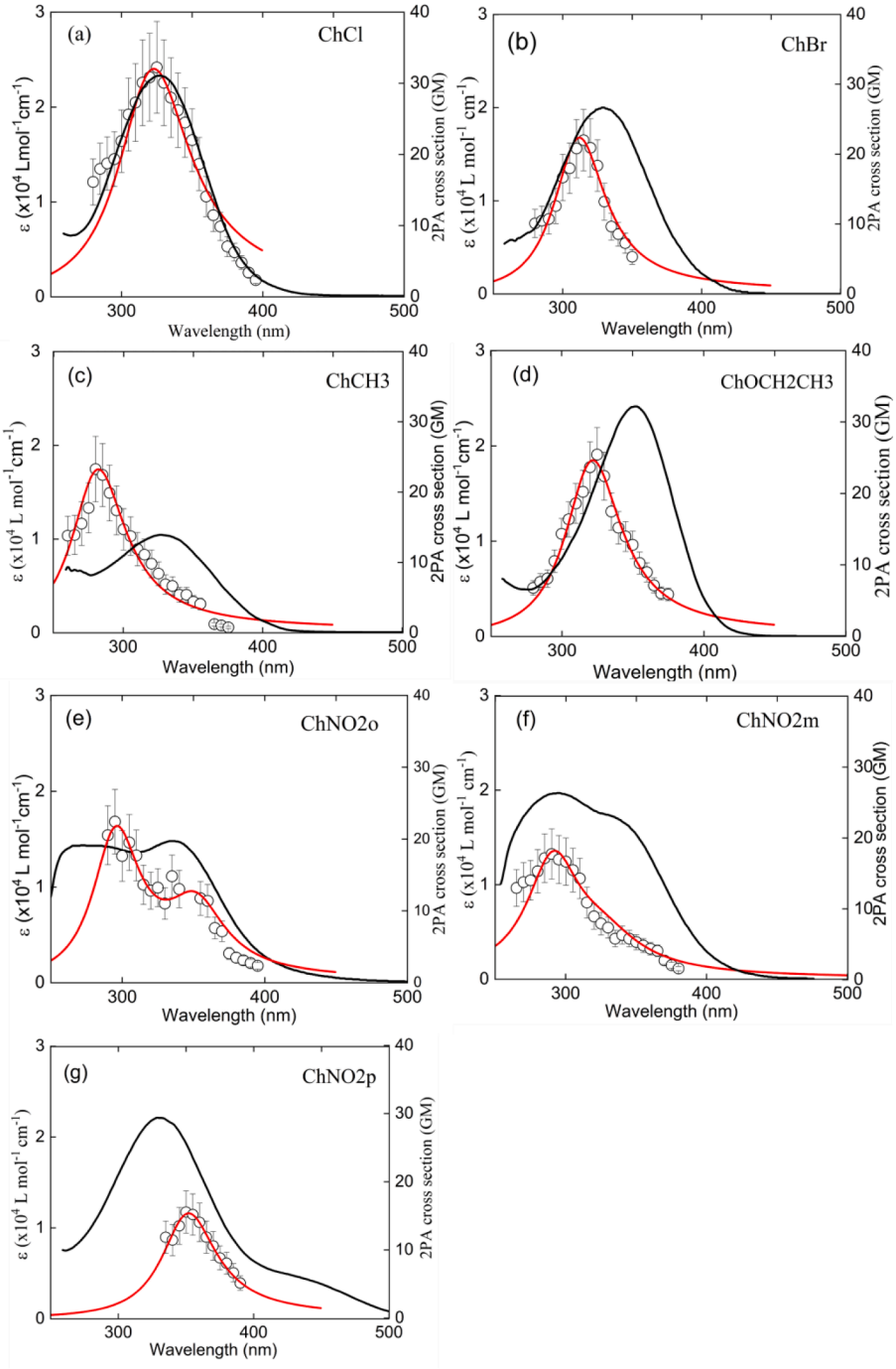

Fig. 5. Molar absorptivity (black lines – left axes) and experimental 2PACS (circles – right axes) of terpenoid-like chalcone derivatives in DMSO. The red lines represent the model with SOS approach.

in which ω_{02}, $\Delta\mu_{02}$ and μ_{02} are the angular frequency transition, the dipole moments difference, and the transition dipole moment from the ground to the second excited state, respectively. However, for a three-level-energy system, there is a three-state term (third term in brackets) and an interference term (fourth term in brackets). The former is related to the absorption of the first excited state to the second one, while the latter is related to a mixing of all states involved in the molecular system, which generates interference between them.

The parameters necessary to apply the SOS approach are μ_{01}, μ_{02}, μ_{12}, $\Delta\mu_{01}$ and $\Delta\mu_{02}$. The transition dipole moments μ_{0n} are determined from the linear absorption measurements applying [48,49].

$$\left|\vec{\mu}_{0n}\right|^2 = \frac{3\times 10^3 ln(10)hc}{(2\pi)^3 N_A}\frac{n}{L^2}\frac{1}{\omega_{0n}}\int_{\varepsilon_1}^{\varepsilon_f}\varepsilon(\omega)d\omega \quad (5)$$

where n is the state of interest ($n = 1,2$), N_A is the Avogadro's number, $\int_{\varepsilon_1}^{\varepsilon_f}\varepsilon(\omega)d\omega$ corresponds to the integral of the lower energy band in ε units and ω_{0n} is the angular frequency transition. The values obtained for μ_{0n} are listed in Table 3. $\Delta\mu_{01}$, $\Delta\mu_{02}$ and μ_{12} are obtained by fitting the SOS model to the experimental data (red line in Fig. 5). The parameters obtained from the SOS model are presented in Table 2.

The SOS results (Table 2) reveal high values of$\Delta\mu_{01}$, which is a characteristic of non-centrosymmetric compounds. Regarding **Group 1**,

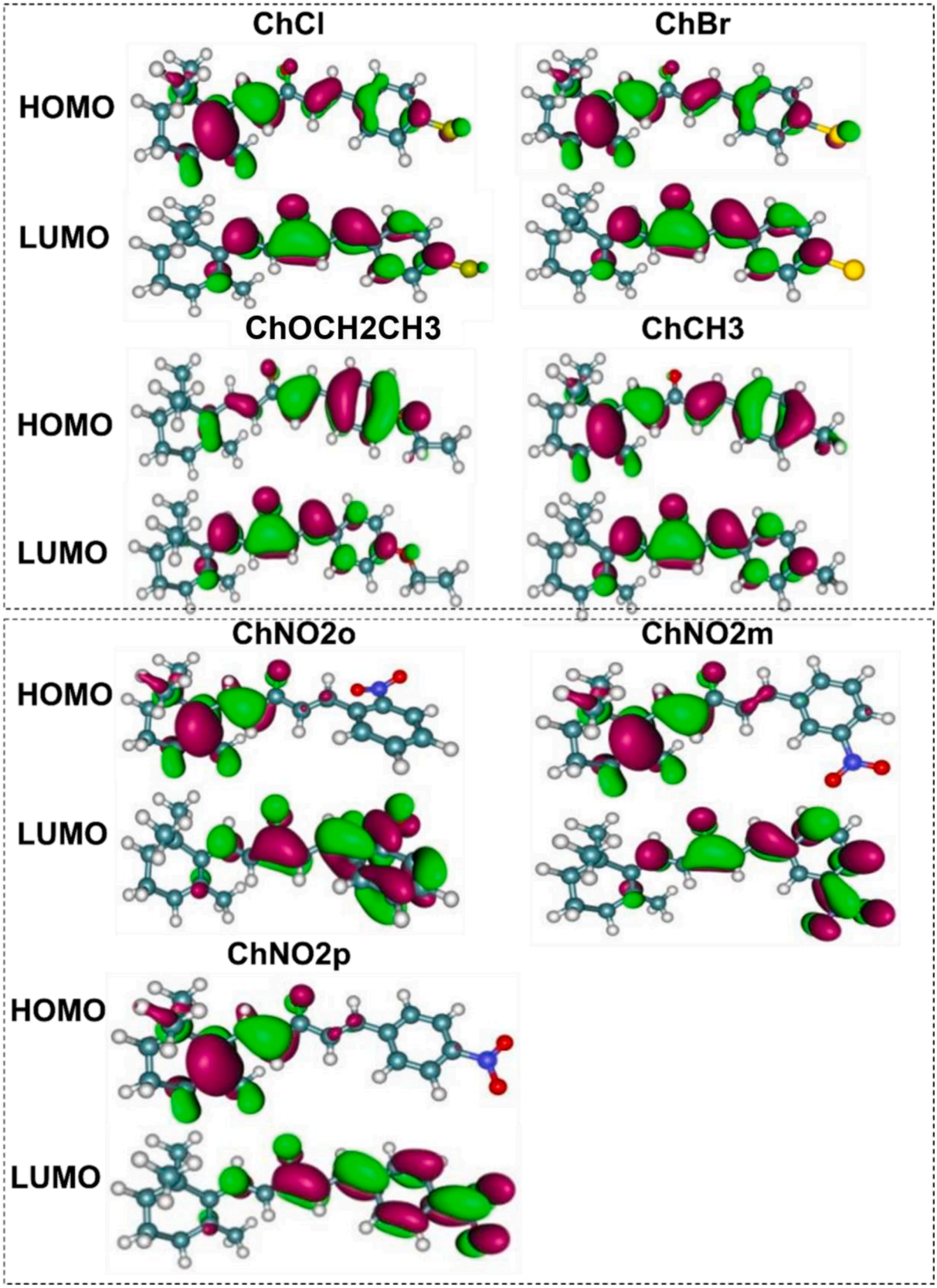

Fig. 6. The frontier molecular orbitals of terpenoid-like chalcone derivatives in DMSO.

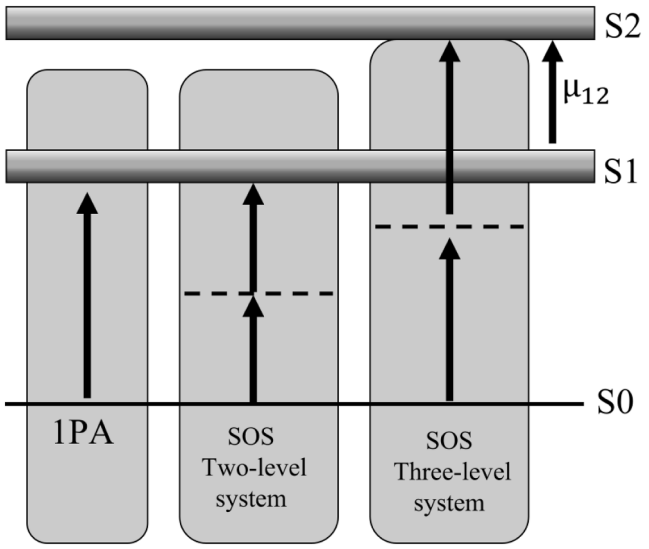

Fig. 7. The representative state diagram for two and three states considered in the SOS approach and.

it is observed that when electron-acceptor groups instead of electron-donating ones are grafted at terpenoid-like chalcone backbone, lower values of $\Delta\mu_{01}$ were observed (see Table 2), indicating that the charge displacement in the first excited state is higher for all D-π-A-D-like architecture. Considering **Group 2**, it is observed that $\Delta\mu_{01}$ scales from ortho to para-position, with meta as intermediary value, which can be related to structural changes caused by the distinct substitutions.

Hyper-Rayleigh scattering was used to explore the first hyperpolarizability (β) of the terpenoid-like chalcone derivatives studied in this work. Nonlinear scattering at 532 nm was measured upon sample excitation at 1064 nm, i.e., two photons are destroyed to create a more energetic one. Experimentally, the samples are excited at 1064 nm with an intensity $I(\omega)$, while the intensity of $I(2\omega)$ of the light scattered at 532 nm is collected. The quadratic dependence between $I(\omega)$ and $I(2\omega)$, as can be seen in the insets of Fig. 8, reveals the second-order nature of the process. To determine β, the intensity I(2ω) divided by $I^2(\omega)$ is plotted as a function of the concentration of the compound for each sample, as depicted in the inset of Fig. 8.

Results of HRS (see Table 3) shows that for **ChCl** and **ChBr**, which present Cl and Br linked to the chalcone moiety, display similar values of β at 1064 nm. These results agree with previously reported ones [50], in which values of approximately 25 $\times$ 10^{-30} esu were determined for the first hyperpolarizability for chlorine, and brome substituted chalcones. Besides, the sample **ChOCH2CH3**, displays a β value of 33.6 $\times$ 10^{-30} esu [14], revealing that donor-electron groups can considerably increase the nonlinear scattering owing to the A-π-D molecular arrangement. This value is in the same order magnitude as the best results found for chalcones derivates [11,22]. Regarding **Group 2** compounds, see Fig. 8 (b), one can note an increase of the second-order molecular hyperpolarizability magnitude when the NO_2 radical is changed from *orto* to *para* position, indicating an increase of effective conjugation length. This result was expected as SOS results displayed higher value of $\Delta\mu_{01}$ for **ChNO2p** derivative.

The first hyperpolarizability can be modeled by applying a

Table 2
Linear and nonlinear optical parameters determined. The superscript *SOS* on the dipole moments difference was placed to highlight such values were obtained from the SOS fitting to the experimental data.

	ChCl	ChBr	ChCH3	ChOCH3	ChNO2o	ChNO2m	ChNO2p
$\lambda_{01}(nm)$	327	329	329	352	337	326	440
$\lambda_{02}(nm)$	–	–	–	–	280	292	330
μ_{01}(D)	6.2 ± 0.6	5.9 ± 0.6	4.2 ± 0.4	5.2 ± 0.5	3.6 ± 0.4	3.8 ± 0.4	1.4 ± 0.1
$\Delta\mu_{01}^{SOS}$(D)	12 ± 2	9 ± 2	15 ± 3	12 ± 2	9.1 ± 3	9.7 ± 3	13.9 ± 2
μ_{02}(D)	–	–	–	–	6.2 ± 0.6	7.0 ± 0.7	7.9 ± 0.8
$\Delta\mu_{02}^{SOS}$(D)	–	–	–	–	3.3 ± 0.6	3.4 ± 0.2	2.6 ± 0.3
μ_{12}(D)	–	–	–	–	6.5 ± 1	5.9 ± 0.4	7.0 ± 0.3

Table 3
Experimental first hyperpolarizability at 1064 nm (β) for all compounds studied in this work.

	ChCl	ChBr	ChCH3	ChOCH3	ChNO2o	ChNO2m	ChNO2p
$\beta(\times 10^{-30} esu)$	22 ± 4	20 ± 4	22 ± 4	33 ± 6	21 ± 4	28 ± 6	39 ± 8

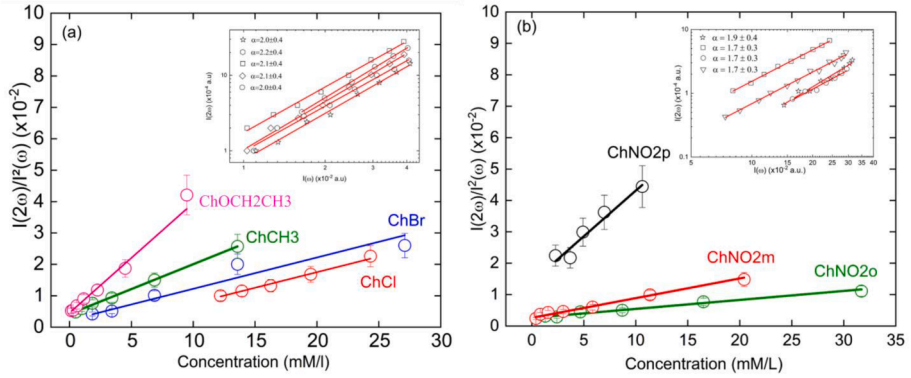

Fig. 8. The linear fitting to obtain $\alpha^{chalcone}$ of each sample for a) group 1 and b) group 2. Besides, the graphs' inset displayed the quadratic relationship between I(2ω) and I(ω) for a) ChCl and b) ChNO2p, for instance.

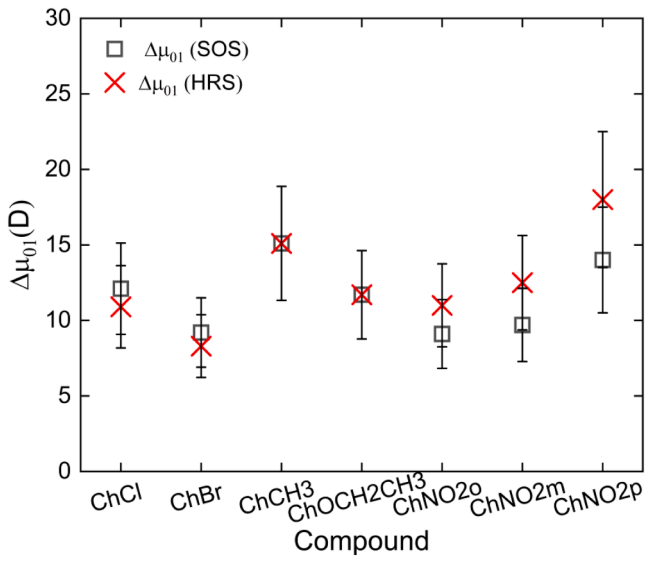

Fig. 9. Comparison of $\Delta\mu_{01}$ values obtained through 2PA (SOS) and HRS modeling of the experimental results for the compounds studied here.

phenomenological approach [51] that considers an undamped two-level system, considering the resonant enhancement effect that appears when the excitation energy approaches the first electronic transition. According to this model,.

$$\beta(-2\omega;\omega,\omega) = \frac{\omega_{01}^4}{(\omega_{01}^2-4\omega^2)(\omega_{01}^2-\omega^2)}\left[\frac{3}{2}\frac{|\mu_{01}|^2|\Delta\mu_{01}^{HRS}|}{(\hbar\omega_{01})^2}\right] \quad (6)$$

in which $\beta(-2\omega;\omega,\omega)$ is the dynamical scattering coefficient (dispersion of the first hyperpolarizability), ω_{01} is the transition frequency, ω is the excitation frequency, μ_{01} is the transition dipole moment, determined from the linear absorption spectrum, and $|\Delta\mu_{01}^{HRS}|$ is the difference of dipole moment between states. Therefore, we can model the experimental results of β at 1064 nm, with $\Delta\mu_{01}^{HRS}$ as the only free parameter and compare its values with the ones obtained from the SOS approach. In Fig. 9 we plot the values of $\Delta\mu_{01}$ obtained by modeling the HRS data ($\Delta\mu_{01}^{HRS}$), as well as the ones found by fitting the 2PACS spectrum using the SOS approach ($\Delta\mu_{01}^{SOS}$).

As it can be seen in Fig. 9, the results of $\Delta\mu_{01}^{HRS}$ and $\Delta\mu_{01}^{SOS}$ are in excellent agreement considering the experimental error. Thus, the analysis of HRS and 2PA measurements, supported by the models, showed a good method to determine $\Delta\mu_{01}$ of non-fluorescent compounds (for fluorescent compounds, usually, Solvatochromism measurements are performed), and consequently, more information about the photophysics can be clarified.

4. Conclusion

Here it a study was performed on the 2PA cross-section and first hyperpolarizability of terpenoid-like chalcones derivatives with different electron-donating and withdrawing groups. The 2PA cross-section spectrum, determined through the Z-Scan technique, agrees with the SOS approach. The addition of NO_2 group in different positions (**Group 2**) results in a considerable decrease in the 2PA cross-section maximum compared to the other chalcone derivatives (**Group 1**). The NO_2 group is a more effective electron-accepting moiety than C═O, as shown by the QCC. Regarding HRS studies, it was possible to determine β^{HRS} at 1064 nm. Moreover, combining the experimental results with the phenomenological approaches, it was possible to determine $\Delta\mu_{01}$ and compare with the ones obtained through the SOS approach (2PA). Such analysis showed low discrepancy among both results, hence elucidating an excellent route to determine this parameter for non-fluorescent compounds. In conclusion, the present work clarifies the changes in the linear and nonlinear optical properties owing to different peripherical groups on the chalcone backbone, providing a better understanding of this exciting class of organic materials.

CRediT authorship contribution statement

Diego S. Manoel: Writing – original draft, Visualization, Validation, Methodology, Investigation, Formal analysis, Data curation. **André G. Pelosi:** . **Leandro H.Z. Cocca:** Writing – review & editing, Writing – original draft, Methodology, Investigation, Formal analysis. **Gustavo F. B. Almeida:** Methodology, Investigation. **Lucas F. Sciuti:** Software, Methodology. **Ruben D.F. Rodriguez:** Investigation. **Luizmar Adriano Junior:** . **Rosa S. Lima:** Methodology, Investigation. **Caridad Noda-Perez:** Visualization, Resources, Methodology, Investigation. **Felipe T. Martins:** Methodology, Investigation. **Marcio A.R. Souza:** Methodology, Investigation. **Pablo J. Gonçalves:** Writing – review & editing, Writing – original draft, Software, Methodology, Investigation, Formal analysis. **Tertius L. Fonseca:** Writing – review & editing, Writing – original draft, Software, Investigation, Formal analysis. **Leonardo de Boni:** Writing – review & editing, Writing – original draft, Visualization, Validation, Supervision, Software, Resources, Project administration, Methodology, Investigation, Formal analysis, Data curation, Conceptualization. **Cleber R. Mendonça:** .

Declaration of Competing Interest

The authors declare that they have no known competing financial interests or personal relationships that could have appeared to influence the work reported in this paper.

Acknowledgements

The authors gratefully acknowledge financial support from Fundação de Amparo à Pesquisa do Estado de Goiás (FAPEG); Conselho Nacional de Desenvolvimento Científico e Tecnológico (CNPq); Sisfóton/MCTI; Fundação de Amparo à Pesquisa do Estado de São Paulo (FAPESP) - 2018/11283-7; Coordenação de Aperfeiçoamento de Pessoal de Nível Superior (CAPES) - Finance Code 001; Army Research Laboratory (W911NF-17-1-0123) and the Air Force Office of Scientific Research (FA9550-12-1-0028).

Reference

[1] C. Tang, Q. Zheng, H. Zhu, L. Wang, S.-C. Chen, E. Ma, X. Chen, Two-photon absorption and optical power limiting properties of ladder-type tetraphenylene cored chromophores with different terminal groups, J. Mater. Chem. C. 1 (2013) 1771–1780, https://doi.org/10.1039/C2TC00780K.

[2] H. Ftouni, F. Bolze, J.-F. Nicoud, Water-soluble diketopyrrolopyrrole derivatives for two-photon excited fluorescence microscopy, Dye. Pigment. 97 (2013) 77–83, https://doi.org/10.1016/j.dyepig.2012.11.028.

[3] D.S. Correa, M.R. Cardoso, V. Tribuzi, L. Misoguti, C.R. Mendonca, Femtosecond laser in polymeric materials: microfabrication of doped structures and micromachining, IEEE J. Sel. Top. Quantum Electron. 18 (1) (2012) 176–186.

[4] C.R. Mendonca, D.S. Correa, F. Marlow, T. Voss, P. Tayalia, E. Mazur, Three-dimensional fabrication of optically active microstructures containing an electroluminescent polymer, Appl. Phys. Lett. 95 (11) (2009) 113309.

[5] C.C. Corredor, Z.L. Huang, K.D. Belfield, Two-photon 3D optical data storage via fluorescence modulation of an efficient fluorene dye by a photochromic diarylethene, Adv. Mater. 18 (2006) 2910–2914, https://doi.org/10.1002/adma.200600826.

[6] C.R. Mendonça, U.M. Neves, L. De Boni, A.A. Andrade, D.S. dos Santos, F. J. Pavinatto, S.C. Zilio, L. Misoguti, O.N. Oliveira, Two-photon induced anisotropy in PMMA film doped with Disperse Red 13, Opt. Commun. 273 (2) (2007) 435–440, https://doi.org/10.1016/J.OPTCOM.2007.01.035.

[7] M. Velusamy, J.-Y. Shen, J.T. Lin, Y.-C. Lin, C.-C. Hsieh, C.-H. Lai, C.-W. Lai, M.-L. Ho, Y.-C. Chen, P.-T. Chou, J.-K. Hsiao, A new series of quadrupolar type two-photon absorption chromophores bearing 11, 12-dibutoxydibenzo[a, c]-phenazine bridged amines; their applications in two-photon fluorescence imaging and two-photon photodynamic therapy, Adv. Funct. Mater. 19 (2009) 2388–2397, https://doi.org/10.1002/adfm.200900125.

[8] S.R. Lemes, L.A. Júnior, D. da Silva Manoel, M.A.M. de Sousa, R.D. Fonseca, R. S. Lima, C. Noda-Perez, P.R. de Melo Reis, C.G. Cardoso, E. de Paula Silveira-Lacerda, M.A.R. Souza, C.R. Mendonça, P.J. Gonçalves, L. de Boni, T.L. da Fonseca, N.J. da Silva Junior, Optical properties and antiangiogenic activity of a chalcone derivate, Spectrochim. Acta. A. Mol. Biomol. Spectrosc. 204 (2018) 685–695, https://doi.org/10.1016/j.saa.2018.06.099.

[9] J.M.F. Custodio, G.D.C. D'Oliveira, F. Gotardo, L.H.Z. Cocca, L. De Boni, C. N. Perez, L.J.Q. Maia, C. Valverde, F.A.P. Osório, H.B. Napolitano, Chalcone as potential nonlinear optical material: a combined theoretical, structural, and spectroscopic study, J. Phys. Chem. C. 123 (2019) 5931–5941, https://doi.org/10.1021/acs.jpcc.9b01063.

[10] J. Custodio, F. Gotardo, W. Vaz, G. D'Oliveira, L.H. Cocca, R. Fonseca, N. P. Caridad, L. Boni, H. Napolitano, Sulphonamide chalcones: conformationally diverse yet optically similar, J. Mol. Struct. 1198 (2019), 126896, https://doi.org/10.1016/j.molstruc.2019.126896.

[11] L.M.G. Abegão, F.A. Santos, R.D. Fonseca, A.L.B.S. Barreiros, M.L. Barreiros, P. B. Alves, E.V. Costa, G.B. Souza, M.A.R.C. Alencar, C.R. Mendonça, K. Kamada, L. De Boni, J.J. Rodrigues, Chalcone-based molecules: experimental and theoretical studies on the two-photon absorption and molecular first hyperpolarizability, Spectrochim. Acta Part A Mol. Biomol. Spectrosc. 227 (2020), 117772, https://doi.org/10.1016/j.saa.2019.117772.

[12] J.M.F. Custodio, G.D.C. D'Oliveira, F. Gotardo, L.H.Z. Cocca, L. de Boni, C.N. Perez, H.B. Napolitano, F.A.P. Osorio, C. Valverde, Second-order nonlinear optical properties of two chalcone derivatives: insights from sum-over-states, Phys. Chem. Chem. Phys. 23 (2021) 6128–6140, https://doi.org/10.1039/D0CP06469F.

[13] R.G.M. da Costa, R. de Queiroz Garcia, R.M.d.R. Fiuza, L. Maqueira, A. Pazini, L. de Boni, J. Limberger, Synthesis, photophysical properties and aggregation-induced enhanced emission of bischalcone-benzothiadiazole and chalcone-benzothiadiazole hybrids, J. Lumin. 239 (2021) 118367.

[14] D.S. Corrêa, S.L. Oliveira, L. Misoguti, S.C. Zilio, R.F. Aroca, C.J.L. Constantino, C. R. Mendonça, Investigation of the two-photon absorption cross-section in perylene tetracarboxylic derivatives: nonlinear spectra and molecular structure, J. Phys. Chem. A. 110 (2006) 6433–6438, https://doi.org/10.1021/jp057065e.

[15] B.J. Coe, L.A. Jones, J.A. Harris, B.S. Brunschwig, I. Asselberghs, K. Clays, A. Persoons, Highly unusual effects of π-conjugation extension on the molecular linear and quadratic nonlinear optical properties of ruthenium(II) ammine complexes, J. Am. Chem. Soc. 125 (2003) 862–863, https://doi.org/10.1021/ja028897i.

[16] V. Alain-Rizzo, L. Thouin, M. Blanchard-Desce, U. Gubler, C. Bosshard, P. Gunter, J. Muller, F. Alain, M. Barzoukas, Molecular engineering of push-pull phenylpolyenes for nonlinear optics: improved solubility, stability, and nonlinearities, Adv. Mater. 11 (1999) 1210–1214, https://doi.org/10.1002/(SICI)1521-4095(199910)11:14<1210::AID-ADMA1210>3.0.CO;2-R.

[17] K. Feng, L. De Boni, L. Misoguti, C.R. Mendonça, M. Meador, F.-L. Hsu, X.R. Bu, Y-shaped two-photon absorbing molecules with an imidazole–thiazole core, Chem. Commun. (2004) 1178–1180, https://doi.org/10.1039/B402019G.

[18] S. Nasir Abbas Bukhari, M. Jasamai, I. Jantan, W. Ahmad, Review of methods and various catalysts used for chalcone synthesis, Mini. Rev. Org. Chem. 10 (2013) 73–83, https://doi.org/10.2174/1570193x11310010006.

[19] A.M. Asiri, S.A. Khan, Synthesis and anti-bacterial activities of a bis-chalcone derived from thiophene and its bis-cyclized products, Molecules. 16 (2011) 523–531, https://doi.org/10.3390/molecules16010523.

[20] A. Modzelewska, C. Pettit, G. Achanta, N.E. Davidson, P. Huang, S.R. Khan, Anticancer activities of novel chalcone and bis-chalcone derivatives, Bioorg. Med. Chem. 14 (2006) 3491–3495, https://doi.org/10.1016/j.bmc.2006.01.003.

[21] P.C. Rajesh Kumar, V. Ravindrachary, K. Janardhana, H.R. Manjunath, P. Karegouda, V. Crasta, M.A. Sridhar, Optical and structural properties of chalcone NLO single crystals, J. Mol. Struct. 1005 (1-3) (2011) 1–7, https://doi.org/10.1016/J.MOLSTRUC.2011.07.038.

[22] L.M.G. Abegão, R.D. Fonseca, F.A. Santos, G.B. Souza, A.L.B.S. Barreiros, M. L. Barreiros, M.A.R.C. Alencar, C.R. Mendonça, D.L. Silva, L. De Boni, J. J. Rodrigues, Second- and third-order nonlinear optical properties of unsubstituted and mono-substituted chalcones, Chem. Phys. Lett. 648 (2016) 91–96, https://doi.org/10.1016/J.CPLETT.2016.02.009.

[23] S. Perveen, Introductory chapter: terpenes and terpenoids, in: Terpenes and Terpenoids, IntechOpen, 2018, https://doi.org/10.5772/intechopen.79683.

[24] L.R.L. Diniz, Y. Perez-Castillo, H.A. Elshabrawy, C.d.S.M.B. Filho, D.P. de Sousa, Bioactive terpenes and their derivatives as potential SARS-CoV-2 proteases inhibitors from molecular modeling studies, Biomolecules. 11 (1) (2021) 74.

[25] D.K. Mahapatra, S.K. Bharti, V. Asati, Anti-cancer chalcones: structural and molecular target perspectives, Eur. J. Med. Chem. 98 (2015) 69–114, https://doi.org/10.1016/j.ejmech.2015.05.004.

[26] C. Karthikeyan, N.S.H. Narayana Moorthy, S. Ramasamy, U. Vanam, E. Manivannan, D. Karunagaran, P. Trivedi, Advances in chalcones with anticancer activities, Recent Pat. Anticancer. Drug Discov. 10 (2014) 97–115, https://doi.org/10.2174/1574892809666140819153902.

[27] M.G. Vivas, D.L. Silva, L.d. Boni, R. Zalesny, W. Bartkowiak, C.R. Mendonca, Two-photon absorption spectra of carotenoids compounds, J. Appl. Phys. 109 (10) (2011) 103529.

[28] M. Fujiwara, K. Yamauchi, M. Sugisaki, K. Yanagi, A. Gall, B. Robert, R.J. Cogdell, H. Hashimoto, Large third-order optical nonlinearity realized in symmetric nonpolar carotenoids, Phys. Rev. B. 78 (2008), 161101, https://doi.org/10.1103/PhysRevB.78.161101.

[29] A. Major, F. Yoshino, J.S. Aitchison, P.W.E. Smith, D. Zigmantas, V. Barzda, Picosecond z-scan measurements of the two-photon absorption in beta-carotene solution over the 590-790 nm wavelength range, in: J.G. Grote, T. Kaino, F. Kajzar (Eds.), 2005: p. 269. doi:10.1117/12.590669.

[30] J. Huang, W. Hu, M. Yu, Y. Ren, L. Zhang, H. Yang, Effects of terpene alcohol dopant on the morphology and electro-optical properties of polymer-dispersed liquid-crystal composite films, Polym. Adv. Technol. 32 (2021) 4153–4161, https://doi.org/10.1002/pat.5424.

[31] W.B. Fernandes, L.A. Malaspina, F.T. Martins, L.M. Lião, A.J. Camargo, C. Lariucci, C. Noda-Perez, H.B. Napolitano, Conformational variability in a new terpenoid-like bischalcone: structure and theoretical studies, J. Struct. Chem. 54 (2013) 1112–1121, https://doi.org/10.1134/S0022476613060164.

[32] J.M.F. Custodio, W.F. Vaz, A. Bernardes, A.F. Moura, A.G. Oliver, S. Molnár, P. Perjési, C. Noda-Perez, Alternative mechanisms of action for the apoptotic activity of terpenoid-like chalcone derivatives, New J. Chem. 45 (2021) 15267–15279, https://doi.org/10.1039/D1NJ02086B.

[33] M. Sheik-bahae, A.A. Said, E.W. Van Stryland, High-sensitivity, single-beam n2 measurements, Opt. Lett. 14 (1989) 955–957, https://doi.org/10.1364/OL.14.000955.

[34] M. Sheik-Bahae, A.A. Said, T. Wei, D.J. Hagan, E.w. Van Stryland, Sensitive measurement of optical nonlinearities using a single beam, IEEE J. Quantum Electron. 26 (1990) 760–769, https://doi.org/10.1109/3.53394.

[35] R.S. Lima, C.N. Perez, C.C. da Silva, M.J. Santana, L.H.K. Queiroz Júnior, S. Barreto, M.O. de Moraes, F.T. Martins, Structure and cytotoxic activity of terpenoid-like chalcones, Arab. J. Chem. 12 (2019) 3890–3901, https://doi.org/10.1016/J.ARABJC.2016.02.013.

[36] K. Clays, A. Persoons, Hyper-Rayleigh scattering in solution, Rev. Sci. Instrum. 63 (1992) 3285–3289, https://doi.org/10.1063/1.1142538.

[37] P.L. Franzen, L. Misoguti, S.C. Zilio, Hyper-Rayleigh scattering with picosecond pulse trains, Appl. Opt. 47 (2008) 1443–1446, https://doi.org/10.1364/AO.47.001443.

[38] R.W. Boyd, Nonlinear Optics, 3rd ed., 2008.

[39] Nonlinear Optics of Organic Molecules and Polymers, Nonlinear Opt. Org. Mol. Polym. (2020). doi:10.1201/9780138745493.

[40] E. Cancès, B. Mennucci, J. Tomasi, A new integral equation formalism for the polarizable continuum model: theoretical background and applications to isotropic and anisotropic dielectrics, J. Chem. Phys. 107 (1997) 3032–3041, https://doi.org/10.1063/1.474659.

[41] J. Guo-Zhu, Q. Jie, Dielectric constant of dimethyl sulfoxide-monohydric alcohol mixture solution at the microwave frequency, Fluid Phase Equilib. 365 (2014) 5–10, https://doi.org/10.1016/j.fluid.2013.12.014.

[42] R.G. LeBel, D.A.I. Goring, Density, viscosity, refractive index, and hygroscopicity of mixtures of water and dimethyl sulfoxide, J. Chem. Eng. Data. 7 (1962) 100–101, https://doi.org/10.1021/je60012a032.

[43] J.M.F. Custodio, F. Gotardo, W.F. Vaz, G.D.C. D'Oliveira, L.R. de Almeida, R. D. Fonseca, L.H.Z. Cocca, C.N. Perez, A.G. Oliver, L. de Boni, H.B. Napolitano, Benzenesulfonyl incorporated chalcones: synthesis, structural and optical properties, J. Mol. Struct. 1208 (2020), 127845, https://doi.org/10.1016/j.molstruc.2020.127845.

[44] W.J. Meath, E.A. Power, On the importance of permanent moments in multiphoton absorption using perturbation theory, J. Phys. B At. Mol. Phys. 17 (1984) 763–781, https://doi.org/10.1088/0022-3700/17/5/017.

[45] M.G. Vivas, C.R. Mendonca, Temperature effect on the two-photon absorption spectrum of all-trans-β-carotene, J. Phys. Chem. A. 116 (2012) 7033–7038, https://doi.org/10.1021/jp303789s.

[46] M.G. Vivas, C. Diaz, L. Echevarria, C.R. Mendonca, F.E. Hernández, L. De Boni, Two-photon circular-linear dichroism of perylene in solution: a theoretical-experimental study, J. Phys. Chem. B. 117 (9) (2013) 2742–2747.

[47] L.M.G. Abegão, L.H.Z. Cocca, J.-C. Mulatier, D. Pitrat, C. Andraud, L. Misoguti, C. R. Mendonça, M.G. Vivas, L. De Boni, Effective π-electron number and symmetry perturbation effect on the two-photon absorption of oligofluorenes, Phys. Chem. Chem. Phys. 23 (2021) 18602–18609, https://doi.org/10.1039/D1CP02553H.

[48] L.H. Zucolotto Cocca, A. Pelosi, L.F. Sciuti, L.M.G. Abegão, K. Kamada, S. Piguel, C. Renato Mendonça, L. De Boni, Two-photon brightness of highly fluorescent imidazopyridine derivatives: two-photon and ultrafast transient absorption studies, J. Mol. Liq. 348 (2022), 118379, https://doi.org/10.1016/j.molliq.2021.118379.

[49] A.G. Pelosi, L.H. Zucolotto Cocca, L.M.G. Abegão, L.F. Sciuti, S. Piguel, L. De Boni, C.R. Mendonça, Influence of electron-withdrawing groups in two-photon absorption of imidazopyridines derivatives, Dye. Pigment. 198 (2022), 109972, https://doi.org/10.1016/j.dyepig.2021.109972.

[50] F.A. Santos, L.M.G. Abegão, R.D. Fonseca, A.M. Alcântara, C.R. Mendonça, M. S. Valle, M.A.R.C. Alencar, K. Kamada, L. De Boni, J.J. Rodrigues, Bromo-and chloro-derivatives of dibenzylideneacetone: experimental and theoretical study of the first molecular hyperpolarizability and two-photon absorption, J. Photochem. Photobiol. A Chem. 369 (2019) 70–76, https://doi.org/10.1016/j.jphotochem.2018.10.012.

[51] J.L. Oudar, Optical nonlinearities of conjugated molecules. Stilbene derivatives and highly polar aromatic compounds, J. Chem. Phys. 67 (1977) 446–457, https://doi.org/10.1063/1.434888.